

and fluorescent probes like chlorotetracycline show that the local concentration of bound calcium within the synergids is high when compared with that in adjacent cells (32, 33)—in particular, in the synergids of grass species such as wheat and pearl millet (33). The sperm cells are released from the pollen tube into a degenerating synergid before fusion with the egg and central cells, so the calcium concentration in the medium surrounding the fusing gametes may be high, and our *in vitro* conditions may thus reflect those *in vivo* conditions.

Under our conditions, fusion seems to be mainly restricted to sperm and egg cell protoplasts. This fusion specificity suggests that cell recognition is preserved. Thus, this kind of *in vitro* fusion system should allow studies of gametic recognition, barriers to cross-species fertilization, the mechanism of gametic fusion, and intracellular signals after fusion. These experiments also provide the possibility of investigating the cellular and molecular biology of the single cell zygote. In particular, the integration of the male nucleus and cytoplasm, and other postfertilization events, such as modifications to the cytoskeleton, can be studied.

REFERENCES AND NOTES

- J. A. Callow, C. J. Stafford, J. R. Green, in *Perspectives in Plant Cell Recognition*, J. A. Callow and J. R. Green, Eds. (Cambridge Univ. Press, Cambridge, 1992), pp. 19–31; K. R. Foltz and W. J. Lennarz, *Dev. Biol.* **158**, 46 (1993).
- D. G. Myles, *Dev. Biol.* **158**, 35 (1993).
- M. Whitaker and K. Swann, *Development* **117**, 1 (1993).
- L. A. Jaffe, *Nature* **261**, 68 (1976); S. H. Brawley, *Dev. Biol.* **144**, 94 (1990).
- M. Veron, C. Foerder, E. M. Eddy, B. M. Shapiro, *Cell* **10**, 321 (1977).
- S. G. Nawaschin, *Bull. Acad. Imp. Sci. St. Petersburg* **8**, 345 (1898); L. Guignard, *Rev. Gen. Bot.* **11**, 129 (1899).
- S. D. Russell, *Int. Rev. Cytol.* **140**, 357 (1992).
- C. H. Theunis, E. S. Pierson, M. Cresti, *Sex. Plant Reprod.* **4**, 145 (1991).
- E. Kranz, J. Bautor, H. Lörz, *ibid.*, p. 12.
- J.-E. Faure, H. L. Mogensen, C. Dumas, H. Lörz, E. Kranz, *Plant Cell* **5**, 747 (1993).
- E. Kranz and H. Lörz, *ibid.*, p. 739.
- R. Chasan, *ibid.*, p. 718; B. Goodman, *Science* **261**, 430 (1993).
- E. Kranz, J. Bautor, H. Lörz, *Sex. Plant Reprod.* **4**, 17 (1991).
- Maize plants (*Zea mays* L.) of inbred line A188 were grown in a regulated growth chamber at the Université Claude Bernard, Lyon, France. The temperature ranged from 25°C (day) to 19°C (night), with a 16-hour photoperiod at 70 to 90% relative humidity and a light intensity of 700 to 750 $\mu\text{mol m}^{-2} \text{s}^{-1}$, provided by high-pressure sodium lamps (Sodiciaude 1000 W, Claude, Tinen, Belgium). To prevent pollination, the ears used for female protoplast isolation were bagged before silk emergence. The ears were collected at a receptive stage when the emerged silks were 13 to 14 cm long.
- I. Dupuis, P. Roedel, E. Matthys-Rochon, C. Dumas, *Plant Physiol.* **85**, 876 (1987).
- V. T. Wagner, Y. C. Song, E. Matthys-Rochon, C. Dumas, *Plant Sci.* **59**, 127 (1989).
- Female gametes were isolated as follows: Ovule pieces containing embryo sacs were removed from the ovaries and incubated in 1% pectinase (Serva, Heidelberg, Germany), 0.33% pectolyase (Sigma Chimie, St. Quentin Fallavier, France), 0.67% macerozyme Onozuka R10 (Yakult Honsha, Tokyo, Japan), and 0.67% cellulase Onozuka R10 (Yakult Honsha), pH 5.0, adjusted to 550 mosM with mannitol. Ovule pieces were treated for about 25 min at room temperature. Egg cells and central cells were then isolated from the ovule pieces by microdissection with glass microneedles (21) under an inverted IM 35 Zeiss microscope (Oberkochen, Germany).
- The pH was 6 to 6.5. We measured pH using Neutralit pH indicator strips (Merck, Darmstadt, Germany).
- The fusion medium was very slightly diluted with 0.5 M mannitol when the gametes were introduced into it. Probably up to 1/20th of the fusion droplet volume was added with the gametes.
- H.-G. Schweiger *et al.*, *Theor. Appl. Genet.* **73**, 769 (1987).
- We used GC 150-15 glass tubes (Clark Electromedical Instruments, Pangbourne Reading, United Kingdom) to prepare microcapillaries and microneedles. To obtain microcapillaries, we pulled glass tubes manually over a Bunsen burner and cut them with a microforge (Alcatel CIT, Malakoff, France) at a tip diameter of about 100 μm . To obtain microneedles, we pulled glass tubes with a P-80 PC micropipette puller (Sutter Instrument, San Rafael, CA) and sealed their tips with the microforge.
- We define adhesion as a step during which gametes appear to be attached and can be moved together.
- We recorded the fusions with a Sony DXC-107P charge-coupled device color video camera (Sony) mounted on the inverted microscope and with a Panasonic NV-FS 100 HF videocassette recorder (Matsushita Electric Industrial, Osaka, Japan). We obtained pictures by digitizing the video recordings with a Macintosh IICI computer (Apple, Cupertino, CA) equipped with a 24 MxTv video digitizing board (Rasterops, Santa Clara, CA) and then printing the pictures with a Personal Laserwriter (Apple).
- R. Yanagimachi, *Biol. Reprod.* **19**, 949 (1978).
- J.-E. Faure, unpublished results.
- DAPI (4', 6-diamidino-2-phenylindole) is a fluorescent binding probe for DNA. We prepared a staining solution of 14 μM DAPI (Sigma Chimie, St. Quentin Fallavier, France) in 0.5 M mannitol. The apposed gametes and the fusion products were introduced in staining solution droplets of about 3 to 4 μl by use of the microcapillary transfer system (21) and observed under an inverted IM 35 microscope equipped for fluorescence study.
- R. Mòl, E. Matthys-Rochon, C. Dumas, *Plant J.* **5**, 197 (1994).
- Maize seedlings from the inbred line A188 were grown in sterile conditions for 7 days at 24°C in darkness. Leaf pieces were incubated for 60 min in the same enzymatic solution as was used for egg cell protoplast isolation (17). The mesophyll protoplasts were washed in 0.5 M mannitol and introduced into the fusion medium with the microcapillary transfer system (21).
- P. K. Hepler and R. O. Wayne, *Annu. Rev. Plant Physiol.* **36**, 397 (1985); R. E. Cleland, S. S. Virk, D. Taylor, T. Björkman, in *Calcium in Plant Growth and Development*, R. T. Leonard and P. K. Hepler, Eds. (American Society of Plant Physiologists, Rockville, MD, 1990), pp. 9–16.
- O. L. Gamborg, J. P. Shyluk, E. A. Shahin, in *Plant Tissue Culture*, T. A. Thorpe, Ed. (Academic Press, New York, 1981), pp. 115–153.
- G. Zhang, M. K. Campenot, L. E. McGann, D. D. Cass, *Plant Physiol.* **99**, 54 (1992); P. Roedel and C. Dumas, *Sex. Plant Reprod.* **6**, 212 (1993).
- B.-Q. Huang and S. D. Russell, *Sex. Plant Reprod.* **5**, 151 (1992); U. K. Tirlapur, J. L. Van Went, M. Cresti, *Ann. Bot.* **71**, 161 (1993).
- R. Chaubal and B. J. Reeger, *Sex. Plant Reprod.* **3**, 98 (1990); *ibid.* **5**, 34 (1992); *ibid.*, p. 206.
- We thank M. Beckert (Institut National de la Recherche Agronomique, Domaine de Crouelle, Clermont-Ferrand, France) for maize seeds, R. Blanc for growing the maize plants, M. de Barros Lopes for comments on the manuscript, and P. Audenis for photography. Supported by CNRS, INRA, and ENS Lyon.

22 October 1993; accepted 21 January 1994

Biodegradable Long-Circulating Polymeric Nanospheres

Ruxandra Gref,* Yoshiharu Minamitake,†
 Maria Teresa Peracchia,‡ Vladimir Trubetskoy,§
 Vladimir Torchilin,§ Robert Langer||¶

Injectable nanoparticulate carriers have important potential applications such as site-specific drug delivery or medical imaging. Conventional carriers, however, cannot generally be used because they are eliminated by the reticulo-endothelial system within seconds or minutes after intravenous injection. To address these limitations, monodisperse biodegradable nanospheres were developed from amphiphilic copolymers composed of two biocompatible blocks. The nanospheres exhibited dramatically increased blood circulation times and reduced liver accumulation in mice. Furthermore, they entrapped up to 45 percent by weight of the drug in the dense core in a one-step procedure and could be freeze-dried and easily redispersed without additives in aqueous solutions.

The development of intravenously administered carriers with blood circulation times long enough to continuously deliver drugs, imaging agents, or other entities to specific sites of action has been a major challenge. The desired features of such a carrier include (i) that the agent to be encapsulated comprises a reasonably high weight fraction

(loading) of the total carrier system (for example, more than 30%), (ii) that the amount of agent used in the first step of the encapsulation process is incorporated into the final carrier (entrapment efficiency) at a reasonably high level (for example, more than 80%), (iii) the ability to be freeze-dried and reconstituted in solution without

aggregation, (iv) biodegradability, (v) small size (less than 5 μm), and (vi) characteristics to prevent rapid clearance of the particles from the bloodstream. For example, albumin or galactose microspheres used in clinical studies for imaging are cleared from the blood within 20 s, preventing their use in many imaging applications (1). Some progress has been made in reducing the rapid clearance of microparticulates, for example, by the attachment of poloxamer or polysorbate to nondegradable polystyrene or polymethylmethacrylate particles or by the creation of liposomes or other carriers containing glycolipids, albumin, or derivatives of polyethylene glycol (PEG) (2). However, it has been difficult to develop particles displaying all of these qualities. We present here an approach to create degradable polymeric nanospheres that display, to a large extent, the above characteristics.

To form the core of the particles, we used biodegradable materials shown to be safe in the human body such as poly(lactic-co-glycolic acid) (PLGA), polycaprolactone (PCL), and their copolymers (3). By the adjustment of the chemical composition and molecular weight (MW) of a polymer, the degradation time of the core and release kinetics of the encapsulated agent can be controlled (4). To obtain a coating that might prevent opsonization and subsequent recognition by the macrophages of the reticulo-endothelial system, PEG was covalently attached to the nanosphere core by the synthesis of amphiphilic diblock copolymers, PEG-R, where R is one of the previously mentioned biodegradable materials. These diblock copolymers contain groups of ethylene glycol (-EG-EG-EG-) attached together, and this entire block is then bound to a second block of repetitive sequences of monomers such as lactic or glycolic acid or caprolactone (forming the more hydrophobic part of the copolymer, R). We then took advantage of the different solubilities of R (lipophilic) and PEG (hydrophilic) in aqueous and organic solutions to obtain a phase-separated structure.

By using the diblock polymers, we were able to form nanospheres in a one-step procedure. First, PEG-R was dissolved in an organic solvent (methylene chloride, ethyl acetate, or acetone). Then an emulsion (oil in water) was formed in an aqueous phase by vortexing and sonicating. PEG is soluble in water but not in ethyl acetate or acetone. Conversely, R is not water-soluble but is highly soluble in the organic phase. Consequently, PEG migrates from the droplets' inner core to the water interface, and R remains inside the droplets during emulsifi-

cation. Upon solvent evaporation, the nanosphere core solidifies. As a result of the amphiphilic nature of the diblock polymers, the use of other surfactants (not always biocompatible) can be avoided. The particles can then be recovered by centrifugation and lyophilized without protective additives. Lyophilized nanoparticles are easily redispersed in aqueous solutions. Size distribution measurements by quasi-elastic light scattering (QELS) before and after lyophilization established that aggregation does not occur.

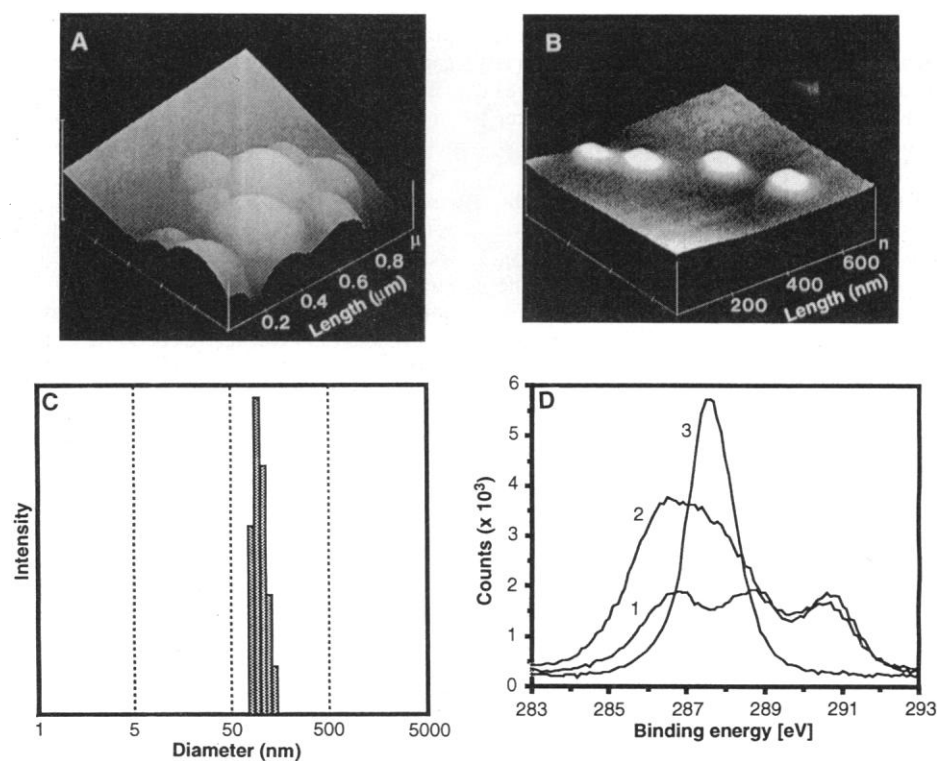


Fig. 1. (A and B) Images of nanospheres taken with an atomic force microscope (Nanoscope III, Digital Instruments, Santa Barbara, California) (scan rate, 2.0 Hz; number of samples, 512). The cantilever oscillates vertically (tapping mode) with a frequency of 350 kHz. (A) PLGA nanospheres (scan size, 1 μm ; set point, 1.6 V; z axis, 250,000 nm per division); (B) PEG-PLGA nanospheres (MW of PEG, 5 kD; MW of PLGA, 45 kD; molar ratio lactic acid:glycolic acid in PLGA, 75:25; scan size, 712.9 nm; set point, 1.7 V; z axis, 100,000 nm per division). The nanospheres were prepared from diblock PLGA-PEG copolymers. These polymers were formed by the direct reaction of the terminal amine group from monoamine, monomethoxy PEG with PLGA (comporting a reactive carboxyl end group). They were also synthesized by the ring-opening polymerization at 114°C of lactide and glycolide in the presence of monomethoxy PEG (weight ratio, 36:9:5), by the use of stannous octoate as a catalyst (0.2 weight percent). Characterization of the polymers by ^{13}C -nuclear magnetic resonance showed that the molar ratio of lactic acid and glycolic acid in PLGA was in each case 3:1 and that the PEG content was approximately 10% by weight. To prepare the nanospheres, a solvent evaporation method (9) was modified for use as follows: The copolymer was first dissolved in an appropriate solvent (ethyl acetate or methylene chloride, 25 mg/2 ml). This solution was poured into 30 ml of distilled water, and an oil-in-water emulsion was formed by vortexing (30 s) and sonicating (1 min, 40-W output). The organic solvent was slowly removed by evaporation at room temperature, under gentle stirring for 2 hours. (C) Quasi-elastic light scattering of PEG-PLGA nanospheres showing unimodal size distribution (mean diameter of 140 nm). Instruments used were a Lexel Argon-ion laser (Fremont, California) (model BI-200SM), with a Brookhaven apparatus consisting of a goniometer and a 136-channel digital correlator and a signal processor. Measurements were made with a laser wavelength of 488 nm at a scattering angle of 90°. (D) Surface chemical analysis (XPS) of (trace 1) PLGA nanospheres, (trace 2) PEG-PLGA nanospheres (MW of PEG, 5 kD; MW of PLGA, 45 kD; and molar ratio of lactic acid:glycolic acid in PLGA, 75:25), and (trace 3) PEG 5 kD crystal powder. Data were collected by MgK α x-rays with a power of 300 W on a Perkin-Elmer 5100 apparatus.

Department of Chemical Engineering, Massachusetts Institute of Technology, Cambridge, MA 02139, USA.

*Present address: ENSIC-LCPM, 1 Rue Grandville, Nancy 54001, France.

†Present address: Suntory Limited, Ohra-Gun, Gunma-Ken 370-05, Japan.

‡Present address: Dipartimento Farmaceutico, Università degli Studi di Parma, Parma 43100, Italy.

§Permanent address: Department of Radiology, Massachusetts General Hospital-East, Charlestown, MA 02129, USA.

||Permanent address: Department of Chemical Engineering, Harvard-Massachusetts Institute of Technology (MIT) Division of Health Sciences, and Whitaker College of Health Sciences, MIT, Cambridge, MA 02139; and Department of Surgery, Children's Hospital, Boston, MA 02115, USA.

¶To whom correspondence should be addressed at MIT, E25-342, Cambridge, MA 02139, USA.

The nanospheres' spherical shape was established by atomic force microscopy (Fig. 1, A and B), a nondestructive technique. The nanospheres are monodispersed, as determined by QELS (Fig. 1C) with a mean diameter between 90 and 150 nm, depending on the type of polymer, MW of PEG, and the organic solvent used.

Surface chemical analysis [x-ray photoelectron spectroscopy (XPS)] performed on lyophilized nanospheres confirmed that the major amount of PEG is concentrated within 5 nm of the outer layer of the nanospheres (Fig. 1D). By comparing XPS spectra before and after incubation in phosphate-buffered saline at 37°C, we found that only a minimal amount of PEG was detached (less than 5% in 24 hours), presumably because of the stability of the ester bond between PEG and R at pH 7.4.

To determine the efficacy of the PEG coating in altering organ distribution of the particles, PEG-coated and noncoated particles were injected into mice (four or five mice per group). Blood circulation time increases as the MW of PEG increases (Fig. 2A). This phenomenon can be explained by an increased thickness of the protective PEG layer, which prevents opsonization. The most striking results were seen in the reduction of liver uptake (Fig. 2B). Only 5 min after injection, 66% of noncoated particles were removed by the liver, while less than 30% of the 20-kD PEG-coated nanospheres were captured by the liver 2 hours after injection. After 5 hours, accumulation of 20-kD PEG-coated nanospheres by the liver still did not exceed 30%.

These dramatic body distribution differences were confirmed by gamma scintigraphy

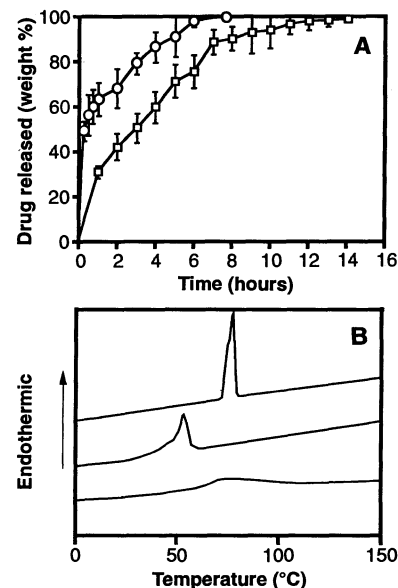
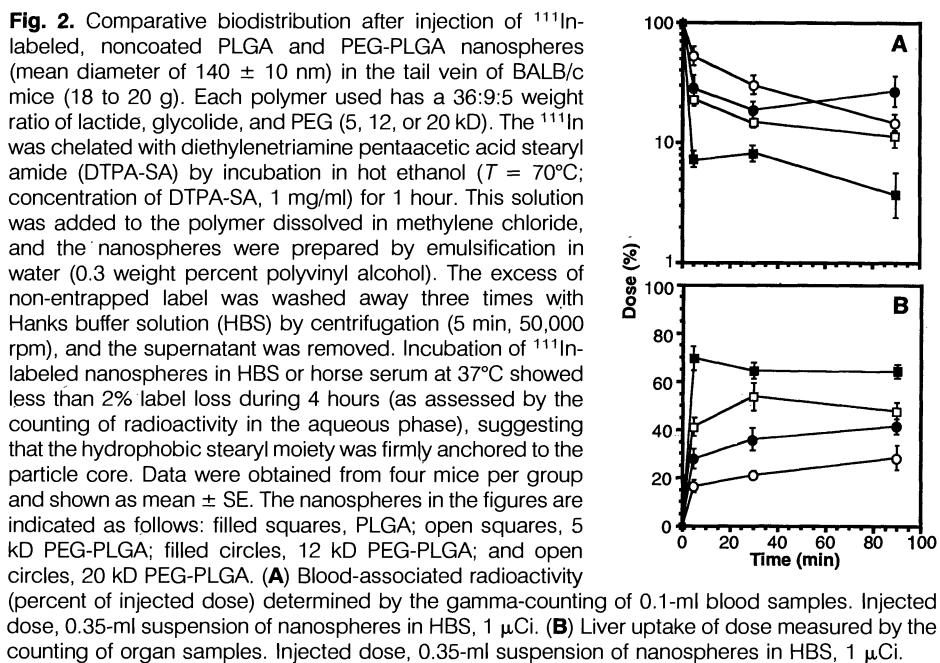
with ^{111}In -labeled particles (three mice per experiment) (5). After 15 min, only liver- and spleen-associated ^{111}In radioactivity was observed with PLGA nanospheres containing no PEG coating. However, high radioactivity was observed in the blood pool (heart and lung) when 20-kD PEG-coated nanospheres of the same size and prepared in the same way were injected, showing the persistence of these particles in the vascular compartment.

To study the encapsulation properties of PEG-coated nanospheres, lidocaine was used as a model drug. Drug-loaded nanospheres were prepared in the same one-step procedure (lidocaine was added to the organic phase, in which the copolymer was dissolved), freeze-dried, and easily dispersed in aqueous phases. High drug loadings (up to 45% by nanosphere weight) and entrapment efficiencies (more than 95% of the initial drug in the encapsulation solution was entrapped) were achieved. Similar loading capacities and entrapment efficiencies were observed for other drugs; for example, prednisolone was encapsulated with nearly identical efficacy. Depending on the properties of the drug (such as charge or hydrophobicity) to be encapsulated, it may be important to alter the solvent system or to use additives to achieve desirable characteristics.

Lidocaine is continually released *in vitro* over 14 hours (Fig. 3A). The release is fast because of the nanosphere's high surface area and small drug size. We observed that the higher the nanoparticle drug content, the slower the release. One explanation for this relation takes into account the possibility of drug crystallization inside the

nanospheres. This hypothesis was supported by calorimetric (Fig. 3B) and x-ray diffraction studies (5). At low loading, lidocaine is present as a molecular dispersion inside the PLGA core. At high loading, a phase separation occurs, leading to the crystallization of part of the drug. The crystallized drug should dissolve and diffuse more slowly into the outer aqueous phase. Control of the drug-release kinetics can presumably be achieved by optimizing the chemical composition of the diblock polymers, the drug loading, and the particle size of the nanospheres (6).

The PEG-coated particles could be used in various ways. By the attachment of an appropriate protein such as transferrin to the surface of the particles (7), endocytosis of a particle containing DNA may be possible. Alternatively, antibodies could be attached to the PEG end group (8), potentially forming highly specific, targetable entities to desired tissues. With further study, these nanospheres may be useful in drug delivery, medical imaging, gene therapy, or a variety of other applications.



REFERENCES AND NOTES

- S. Gottlieb, A. Ernst, L. Litt, K. Q. Schwarz, R. S. Meltzer, *J. Am. Soc. Echocardiography* **3**, 238 (1990); J. R. Saphiro, S. A. Reisner, G. S. Lichtenberg, R. S. Meltzer, *J. Am. Coll. Cardiol.* **16**, 1603 (1990); K. Sugibayashi, Y. Morimoto, T. Nadai, Y. Kato, *Chem. Pharmacol. Bull.* **25**, 3433 (1977).
- V. P. Torchilin *et al.*, *Fed. Am. Soc. Exp. Biol. J.* **6**, 2716 (1992); L. Illum, L. O. Jacobsen, R. H. Müller, R. Mak, S. S. Davis, *Biomaterials* **8**, 113 (1987); J. Lee, P. A. Martic, J. S. Tan, *J. Colloid Interface Sci.* **131**, 252 (1989); D. D. Lasic, F. J. Martin, A. Gabizon, S. K. Huang, D. Papahadjopoulos, *Biochim. Biophys. Acta* **1070**, 187 (1991); M. Donbrow, Ed., *Microcapsules and Nanoparticles in Medicine and Pharmacy* (CRC Press, Boca Raton, FL, 1992); T. M. Allen and C. Hansen, *Biochim. Biophys. Acta* **1068**, 133 (1991); R. H. Müller, K. H. Wallis, S. D. Tröster, J. Kreuter, *J. Controlled Release* **20**, 237 (1992); T. Verrecchia *et al.*, paper presented at VIII Journées Scientifiques du Groupe Thematique de Recherche sur les Vecteurs, Nancy, France, 6 to 10 December 1993; B. G. Müller and T. Kissel, *Pharm. Pharmacol. Lett.* **3**, 67 (1993); D. Bazile *et al.*, *Yanuzaijaku* **53**, 10 (1993).
- A. Schindler *et al.*, *Contemp. Top. Polym. Sci.* **2**, 251 (1977); R. J. Kelly, *Rev. Surg.* **2**, 142 (1970).
- S. W. Kim, R. V. Petersen, J. Feijen, in *Polymeric Drug Delivery Systems*, A. J. Ariens, Ed. (Academic Press, New York, 1992), p. 193.
- R. Gref, Y. Minamitake, M. T. Peracchia, V. Torchilin, R. Langer, unpublished data.
- S. J. Holland, B. J. Tighe, P. L. Gould, *J. Controlled Release* **4**, 155 (1986).
- E. Wagner, M. Zenke, M. Cotten, H. Beug, M. L. Birnstiel, *Proc. Natl. Acad. Sci. U.S.A.* **87**, 3410 (1990).
- G. Blume *et al.*, *Biochem. Biophys. Acta* **1149**, 180 (1993).
- L. R. Beck, V. Z. Pope, D. R. Cowsar, D. H. Lewis, T. R. Tice, *Adv. Contracep. Delivery Syst.* **1**, 79 (1986).
- We thank A. Milshteyn, E. L. Shaw, S. Cohen, A. Domb, G. Wolf, and R. Nanda for assistance. Supported by National Institutes of Health grants U01 CA52857 and GM 26698 and a Lavoisier grant from the French Foreign Affairs Ministry.

6 October 1993; accepted 21 January 1994

Loss of Circadian Behavioral Rhythms and *per* RNA Oscillations in the *Drosophila* Mutant *timeless*

Amita Sehgal,^{*†} Jeffrey L. Price,[†] Bernice Man,[‡] Michael W. Young[§]

Eclosion, or emergence of adult flies from the pupa, and locomotor activity of adults occur rhythmically in *Drosophila melanogaster*, with a circadian period of about 24 hours. Here, a clock mutation, *timeless* (*tim*), is described that produces arrhythmia for both behaviors. The effects of *tim* on behavioral rhythms are likely to involve products of the X chromosome-linked clock gene *period* (*per*), because *tim* alters circadian oscillations of *per* RNA. Genetic mapping places *tim* on the left arm of the second chromosome between *dumpy* (*dp*) and *decapentaplegic* (*dpp*).

Fruit flies show circadian regulation of several behaviors (1, 2). When populations of *Drosophila* are entrained to 12 hours of light followed by 12 hours of darkness (LD 12:12), adults emerge from pupae (eclose) rhythmically, with peak eclosion recurring every morning. The eclosion rhythm persists when the entraining cues are removed and behavior is monitored in constant darkness, thus indicating the existence of an endogenous clock. Adult locomotor activity is also controlled by an endogenous clock and recurs rhythmically with a 24-hour period.

Howard Hughes Medical Institute, National Science Foundation Science and Technology Center for Biological Timing, and Laboratory of Genetics, The Rockefeller University, New York, NY 10021, USA.

^{*}Present address: Department of Neuroscience, University of Pennsylvania School of Medicine, Philadelphia, PA 19104, USA.

[†]These authors contributed equally to this study.

[‡]Present address: Stanford University Medical School, Palo Alto, CA 94305, USA.

[§]To whom correspondence should be addressed.

Several mutations that affect eclosion and locomotor activity have been isolated in behavioral screens (2–4). The best characterized, and those with the strongest phenotypes, are mutations at the X chromosome-linked *period* (*per*) locus (3). Missense mutations at *per* can lengthen or shorten the period of circadian rhythms, whereas null mutations abolish circadian rhythms altogether. The *per* gene is expressed in many cell types at various stages of development. In most cell types, the *period* protein (PER) is found in nuclei (5, 6). A domain within PER is also found in the *Drosophila single-minded* protein (SIM) and in subunits of the mammalian aryl hydrocarbon receptor (7), and this domain (PAS, for PER, ARNT, and SIM) mediates dimerization of PER (8). The amounts of both PER protein and RNA oscillate with a circadian period, which is affected by the *per* mutations in the same manner as behavioral rhythms are affected (6, 9). Given the homologies to *sim* and the aryl

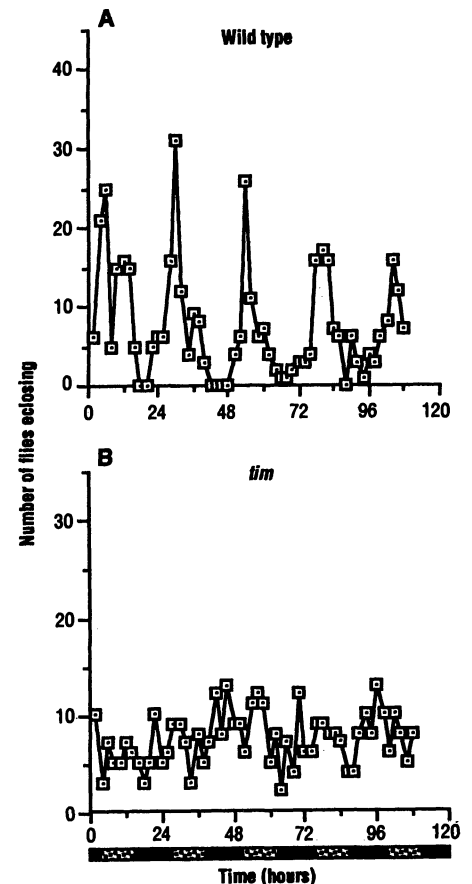


Fig. 1. Assessment of eclosion in *tim* flies. (A) Eclosion of wild-type flies in constant darkness (DD). (B) Eclosion of *tim* flies in DD. At the bottom of (B) are phases of LD cycles during entrainment (hatched boxes represent subjective day during collection). We entrained flies by maintaining them in LD 12:12 at 25°C for 4 days. Twenty hours before the first collection, lights were turned off. Newly emerged adults were collected and counted every 2 hours. A safelight that blocks wavelengths less than 600 nm (15-W bulb with a Kodak GBX-2 filter) was used to collect the eclosing adults.

hydrocarbon receptor (which are thought to regulate transcription), the effects of *per* on behavioral rhythms have been postulated to depend on circadian regulation of gene expression, including that of *per* itself (9). However, neither direct proof of this postulate nor elucidation of *per*'s actual biochemical function has been forthcoming.

Because an analysis of the molecular mechanisms that underlie circadian rhythms requires the identification of other components in the pathway, we conducted a genetic screen in order to isolate new mutations affecting biological rhythms in *Drosophila*. The mutagenesis was based on the mobilization of single P transposable elements, as described (10). The transposase-encoding, $\Delta 2-3$ P element from the Engels 2 strain (11) was used to mobilize a